Enzyme Inhibitors

DOI: 10.1002/anie.200804695

Cation–π Interactions at the Active Site of Factor Xa: Dramatic Enhancement upon Stepwise N-Alkylation of Ammonium Ions**

Laura M. Salonen, Christoph Bucher, David W. Banner, Wolfgang Haap, Jean-Luc Mary, Jörg Benz, Olivier Kuster, Paul Seiler, W. Bernd Schweizer, and François Diederich**

Dedicated to Professor Julius Rebek, Jr. on the occasion of his 65th birthday

Efficient ligands of factor Xa usually feature a more or less preorganized central scaffold which orients two approximately orthogonal vectors to fill the S1 and S4 pockets at the enzyme active site.[1,2] In earlier work, the S1 pocket was mainly occupied by an aromatic ring bearing a basic residue, such as a phenylamidinium substituent, which in the protonated form ion pairs with the side chain of Asp189 at the bottom of the S1 pocket (Figure 1). More recently,[3] neutral, oral bioavailability-mediating chloroaryl and chloroheteroaryl substituents were chosen as S1 vectors, which undergo a close to orthogonal, dipolar C–Cl···C–O(H) interaction[4] with the side chain of Tyr228 also lining the bottom of the S1 pocket. The S4 pocket constitutes an aromatic box, lined by the side chains of Trp215, Tyr99, and Phe174. Many potent inhibitors feature basic amine residues to fill this pocket which, in protonated form, are involved in efficient cation–π interactions.[5,6] By comparing the binding affinity of the quaternary ammonium ion (±)-**1** (inhibition constant K_i = 280 nM; Figure 1) to that of the *tert*-butyl derivative (±)-**2** (K_i = 29000 nM), we determined the increment in the free enthalpy for the cation–π interaction of (±)-**1** in the S4 pocket of factor Xa to be $\Delta\Delta G = 2.8$ kcal mol^{-1}, approximately 0.9 kcal mol^{-1} per aromatic ring.[7] To comprehensively investigate the nature of this interaction, we redesigned our ligand system: The central tricyclic scaffold and the alkylammonium side chain filling the S4 pocket were maintained, but the phenylamidinium residue in (±)-**1** was substituted for a chloroaryl residue to fill the S1 pocket and address the Tyr228 side chain at the bottom of the pocket. Here, we report that this substitution yields highly potent inhibitors of factor Xa, which allow an accurate quantification of the effects of N-alkylation on the strength of the cation–π interactions.

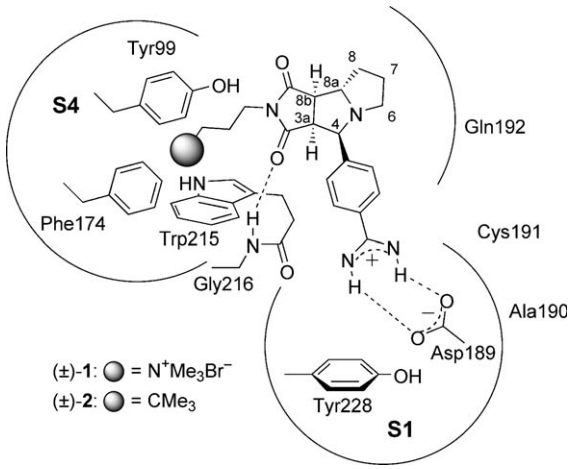

Figure 1. Schematic representation of the active site of factor Xa complexed with the 3a*S*,4*R*,8a*S*,8b*R*-configured enantiomer (*ent*-**1**) of (±)-**1**. X-ray analysis of the cocrystal revealed that only this enantiomer of the *endo*,*trans*-configured cycloadduct is bound.[7] *Exo* and *endo* refer to the orientation of the substituent at C(4) with respect to the bicyclic perhydropyrrolo[3,4-*c*]pyrrole scaffold, while *cis* and *trans* refer to the position of this substituent with respect to the configuration of C(8a) at the fusion of the two pentagons in the perhydropyrrolizidine bicycle.

A search of the Protein Data Bank (PDB) by Relibase[8] for short C–Cl···C–O(H) contacts (< 4 Å) in the S1 pocket of factor Xa yielded 46 hits (Figure SI1 in the Supporting Information). The C···Cl distances vary from 2.9 to 3.9 Å, and the Cl···C–O(H) angles adopt values between 60 and 77°. Molecular modeling studies with the program MOLOC[9] were performed by docking potential new ligands into the active site of factor Xa as seen in the complex with *ent*-**1** (PDB code: 2BOK). This study suggested that the neutral chlorothiophenyl needle of the 3a*S*,4*R*,8a*S*,8b*R*-configured enantiomer of (±)-**3** would properly occupy the S1 pocket, with a dipolar contact with Tyr228 similar to those identified in the PDB search.[3b]

The short synthesis of the *endo*,*trans*-configured ligand (±)-**3** consists of the 1,3-dipolar cycloaddition[10] of maleimide **4** to the azomethine ylide obtained from L-proline (**5**) and aldehyde **6**[11] to give (±)-**7**, followed by nucleophilic substitution with Me_3N (Scheme 1; see the Supporting Information).

The binding activity of (±)-**3** for factor Xa is, with a K_i value in the single-digit nanomolar range (9 nM), strongly enhanced, as compared to the phenylamidinium derivative (±)-**1** (Scheme 1). Cation–π interactions in the S4 pocket are

[*] Dr. D. W. Banner, Dr. W. Haap, J.-L. Mary, Dr. J. Benz, O. Kuster
Pharma Division, Präklinische Forschung
F. Hoffmann-La Roche AG, 4070 Basel (Switzerland)
E-mail: david.banner@roche.com
L. M. Salonen, C. Bucher, P. Seiler, Dr. W. B. Schweizer, Prof. Dr. F. Diederich
Laboratorium für Organische Chemie, ETH Zürich
Hönggerberg, HCI, 8093 Zürich (Switzerland)
Fax: (+41) 44-632-1109
E-mail: diederich@org.chem.ethz.ch

[**] This work was supported by a grant from the ETH Research Council and by F. Hoffmann-La Roche (Basel).

Supporting information for this article is available on the WWW under http://dx.doi.org/10.1002/anie.200804695.

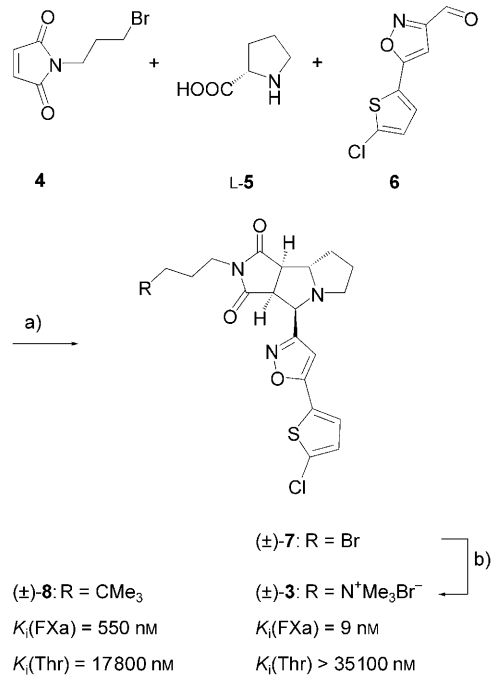

Scheme 1. Synthesis of the inhibitor (±)-**3** (the active enantiomer is shown). a) MeCN, 80 °C, 5 %; b) Me_3N (4.2 M in EtOH), EtOH, 20 °C, 93 %. Also shown are the biological activities (K_i values) of inhibitors (±)-**3** and (±)-**8** against factor Xa and thrombin. (See the Supporting Information for determination of the K_i values and synthesis of (±)-**8**.)

very efficient, as revealed by comparison of the onium ion (±)-**3** with the *tert*-butyl derivative (±)-**8** ($K_i = 550$ nM). The difference in binding affinities $[K_i((\pm)\text{-}\mathbf{8})/K_i((\pm)\text{-}\mathbf{3}) = 61;\ \Delta\Delta G = 2.5\ \text{kcal mol}^{-1}]$, which corresponds to a cation–π interaction of approximately 0.8 kcal mol^{-1} per aromatic ring, is in good accordance with previous findings (see the Supporting Information for the less active *exo*,*trans*-ligands).[5,7,12]

The X-ray crystal structure of (±)-**3** in the complex with factor Xa was solved at 1.25 Å resolution (PDB code: 2JKH; see the Supporting Information). It confirmed, that similar to (±)-**1**, the 3a*S*,4*R*,8a*S*,8b*R*-configured enantiomer (*ent*-**3**) is exclusively bound in the active site (Figure 2). As predicted by modeling studies, the tricyclic scaffold directs the chlorothiophenyl residue into the S1 pocket where it undergoes dipolar interactions with the side chain of Tyr228 [d(Cl···C(OH)) = 3.6 Å, ∢Cl···C–O(H) = 67°]. The quaternary ammonium ion binds in the S4 pocket, where it is located in the center of the aromatic box formed by the side chains of Trp215, Phe174, and Tyr99. The distances between the N^+ center and the closest aromatic C atom [d(N···C–Trp215) = 4.3 Å; d(N···C–Phe174) = 4.7 Å; d(N···C–Tyr99) = 4.8 Å; Figure 2b] correspond well with the values previously determined for *ent*-**1** bound to factor Xa.[7]

The protein as well as the quaternary ammonium center in the aromatic box of the S4 pocket adopt a very similar conformation in the X-ray cocrystal structures of both *ent*-**1** and *ent*-**3** (Figure SI4 in the Supporting Information). In contrast, the rigid tricyclic central scaffold undergoes a truly dramatic repositioning to reach either the Asp189 side chain

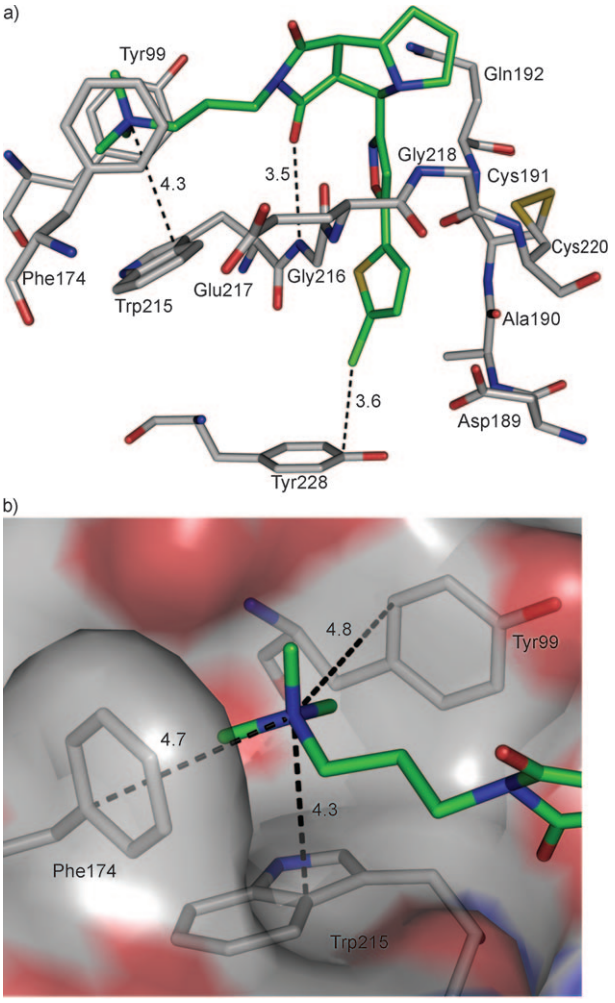

Figure 2. a) Binding mode of inhibitor (3a*S*,4*R*,8a*S*,8b*R*)-**3** in the active site of factor Xa according to the X-ray crystal structure analysis (red O, blue N, yellow S, light green Cl, green C_{ligand}, gray $C_{protein}$; PDB code: 2JKH). b) Closest distances (Å) between the N^+ center and the carbon atoms of the aromatic box in the S4 pocket.

with the phenylamidinium residue, in the case of *ent*-**1**, or the Tyr228 side chain with the chlorothiophenyl residue, in the case of *ent*-**3**. Atoms of the tricyclic scaffold are shifted by up to 6 Å in the two structures (Figure SI5 in the Supporting Information). The bicyclic needle in *ent*-**3** undergoes very efficient π-stacking interactions with the surrounding flat and highly polarizable walls of the S1 pocket, which consists of the backbone of Gly216-Trp215 on one side and Gln192-Cys191-Ala190 on the other (Figure SI6 in the Supporting Information). According to modeling studies, this stacking involves close dipolar contacts such as $S_{thiophene}$···C=O_{Gly216} [d(S···C) = 3.6 Å) and ∢(S···C=O) = 89°], which are more important contributors to the high binding affinity than the dipolar C–Cl···C–O(H) interaction at the bottom of the S1 pocket.[13]

First, we explored the optimal length of the *n*-alkyl spacer connecting the Me_3N^+ ion to the tricyclic imide. Whereas the complexation of (±)-**3** (with a C_3 chain) and (±)-**9** (with a C_4 chain) is equally efficient ($K_i = 9$ nM), ligand (±)-**10** with a longer C_5 spacer is a much weaker binder ($K_i = 146$ nM; Figure 3). For optimal binding, the cation needs to be

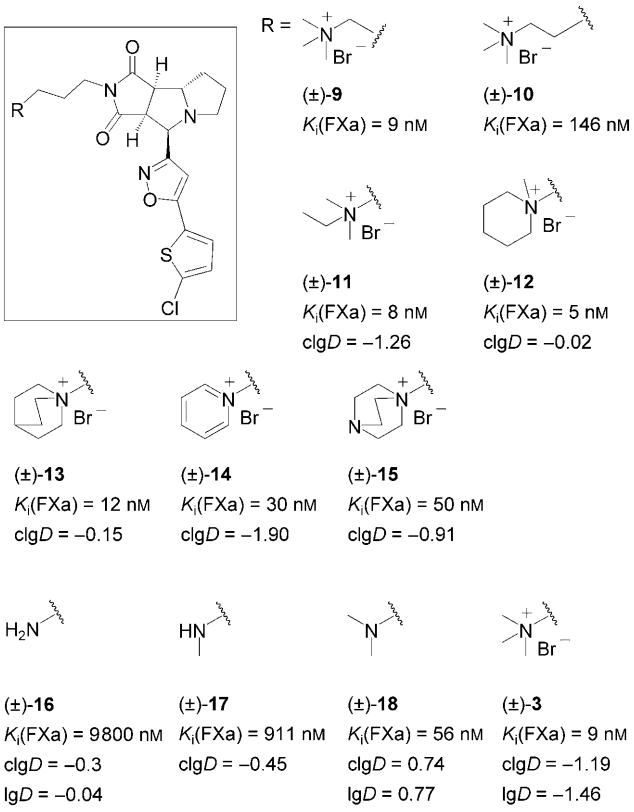

Figure 3. Binding affinity of various ligands for factor Xa. Also shown are the clg$D$ values (calculated logarithmic coefficients for the distribution of a compound between octanol and water at pH 7.4); the experimental lg$D$ values are also given for (±)-**3**, (±)-**16**, and (±)-**18**. A comparison of the selectivities for factor Xa over thrombin is shown in Table SI1 of the Supporting Information.

positioned precisely in the middle of the aromatic box with the N^+ center on the normal passing through the centroids of the aromatic rings, which is possible for (±)-**3** and (±)-**9** but not, without inducing *gauche* strain, for (±)-**10**.

The aromatic box also accepts larger quaternary onium ions: ligands (±)-**11** (ethyldimethylammonium), (±)-**12** (*N*-methylpiperidinium), and (±)-**13** (quinuclidinium) feature high binding affinities, with K_i values between 5 and 12 nM. Introducing a flatter *N*-pyridinium ion[14] ((±)-**14**) decreases the inhibition to 30 nM, and monoquaternized DABCO (1,4-diazabicyclo[2.2.2]octane) also binds less well ((±)-**15**, K_i = 50 nM). Some of these minor changes in affinity could also result from alterations in hydrophobicity; the corresponding logarithmic distribution coefficients (clg$D$) are shown in Figure 3.

A dramatic finding in this study is the dependence of the magnitude of the cation–π interactions on the degree of N-methylation of the terminal amine. In studies on cation–π interactions between differently N-methylated lysine side chains and the indole ring of a tryptophan in a β-hairpin peptide, Waters and co-workers[15] measured an enhancement in the interaction of 0.2–0.3 kcal mol^{-1} for each additional *N*-methyl group. We prepared the primary amine (±)-**16**, secondary amine (±)-**17**, and tertiary amine (±)-**18**, which under the conditions of the biological assay at pH 7.8 are fully protonated, and compared their activity to that of (±)-**3**.

The primary ammonium ion (±)-**16** is a poor binder (K_i = 9800 nM, lg$D$ = –0.04); its affinity for factor Xa is much lower than that of the *tert*-butyl derivative (±)-**8** (K_i = 550 nM). The binding affinity increases with each additional methyl group, with the secondary ammonium ion (±)-**17** still being a modest binder (K_i = 911 nM). A strong increase in the binding affinity is observed upon further methylation to the tertiary ammonium ion (±)-**18** (K_i = 56 nM, lg$D$ = 0.77) and ultimately to the quaternary ammonium ion (±)-**3** (K_i = 9 nM, lg$D$ = –1.46). In the case of the primary and secondary ammonium ions, desolvation of three ((±)-**16**) and two ((±)-**17**) N^+H residues must occur upon insertion into the aromatic box, and these desolvation costs are not recovered by the gain in cation–π interactions. The much stronger binding of the tertiary ammonium ion (±)-**18** is in agreement with the results of our previous PDB search:[7] while the three alkyl residues undergo favorable C–H···π interactions in the molecular box, the N^+H residue reaches outside of the box where it is presumably solvated by one or more water molecules, which are hydrogen-bonded to the protein. On average, the gain in the binding free enthalpy amounts to an increment of $\Delta\Delta G$ = 1.2–1.8 kcal mol^{-1} per methylation. This corresponds to a value of $\Delta\Delta G$ = 0.4–0.6 kcal mol^{-1} per aromatic ring. While increases in lipophilicity upon N-methylation certainly also make a contribution to the enhancement in affinity, the clg$D$ data (Figure 3) clearly show it to be a rather minor factor.

In summary, the cation–π interaction in the complex of factor Xa with (±)-**3** was quantified as $\Delta\Delta G$ = 2.5 kcal mol^{-1}, which corresponds to an interaction of approximately 0.8 kcal mol^{-1} per aromatic ring. The X-ray structures of the cocrystals revealed that the rigid tricyclic central scaffold in bound *ent*-**3** undergoes a dramatic repositioning compared to the same scaffold in the complex of (±)-**1**. Stepwise N-methylation, from the primary ammonium ion (±)-**16** to the quaternary onium ion (±)-**3**, results in the binding affinity increasing by a factor of 1000 ($\Delta\Delta G$ = 4.3 kcal mol^{-1}), which corresponds to an increment in the free enthalpy of $\Delta\Delta G$ = 1.2–1.8 kcal mol^{-1} per methylation. In particular, the poor binding of the primary ammonium ion (±)-**16** leads us to discount cation–π interactions between the side chains of Lys and Trp.[16] Lys and Trp residues preferentially interact by undergoing C–H···π interactions between their side chains. Such interactions are enhanced by the electron-withdrawing effect of the terminal primary ammonium ion, which most probably turns away from the indole surfaces to benefit from better solvation.[15]

Received: September 25, 2008
Published online: December 19, 2008

Keywords: dipolar interactions · enzymes · inhibitors · molecular recognition · pi interactions

[1] a) A. G. G. Turpie, *Arterioscler. Thromb. Vasc. Biol.* **2007**, *27*, 1238–1247; b) S. Haas, *J. Thromb. Thrombolysis* **2008**, *25*, 52–60.

[2] a) S. Roehrig, A. Straub, J. Pohlmann, T. Lampe, J. Pernerstorfer, K.-H. Schlemmer, P. Reinemer, E. Perzborn, *J. Med. Chem.*

2005, *48*, 5900 – 5908; b) D. J. P. Pinto, M. J. Orwat, S. Koch, K. A. Rossi, R. S. Alexander, A. Smallwood, P. C. Wong, A. R. Rendina, J. M. Luettgen, R. M. Knabb, K. He, B. Xin, R. R. Wexler, P. Y. S. Lam, *J. Med. Chem.* **2007**, *50*, 5339 – 5356; c) F. Kuo, D. K. Clodfelter, T. R. Priest, D. L. K. Kau, *J. Labelled Compd. Radiopharm.* **2004**, *47*, 599 – 608; d) R. M. Scarborough, J. P. Kanter, K. Sujino, S. S. Zuberi, WO 2008/057972A1, **2008**; e) K. R. Guertin, C. J. Gardner, S. I. Klein, A. L. Zulli, M. Czekaj, Y. Gong, A. P. Spada, D. L. Cheney, S. Maignan, J.-P. Guilloteau, K. D. Brown, D. J. Colussi, V. Chu, C. L. Heran, S. R. Morgan, R. G. Bentley, C. T. Dunwiddie, R. J. Leadley, H. W. Pauls, *Bioorg. Med. Chem. Lett.* **2002**, *12*, 1671 – 1674; f) T. Furugohri, K. Isobe, Y. Honda, C. Kamisato-Matsumoto, N. Sugiyama, T. Nagahara, Y. Morishima, T. Shibano, *J. Thromb. Haemostasis* **2008**, *6*, 1542 – 1549.

[3] a) Y. M. Choi-Sledeski, R. Kearney, G. Poli, H. Pauls, C. Gardner, Y. Gong, M. Becker, R. Davis, A. Spada, G. Liang, V. Chu, K. Brown, D. Collussi, R. Leadley, S. Rebello, P. Moxey, S. Morgan, R. Bentley, C. Kasiewski, S. Maignan, J.-P. Guilloteau, V. Mikol, *J. Med. Chem.* **2003**, *46*, 681 – 684; b) S. Maignan, J.-P. Guilloteau, Y. M. Choi-Sledeski, M. R. Becker, W. R. Ewing, H. W. Pauls, A. P. Spada, V. Mikol, *J. Med. Chem.* **2003**, *46*, 685 – 690; c) M. Adler, M. J. Kochanny, B. Ye, G. Rumennik, D. R. Light, S. Biancalana, M. Whitlow, *Biochemistry* **2002**, *41*, 15514 – 15523.

[4] R. Paulini, K. Müller, F. Diederich, *Angew. Chem.* **2005**, *117*, 1820 – 1839; *Angew. Chem. Int. Ed.* **2005**, *44*, 1788 – 1805.

[5] a) N. Zacharias, D. A. Dougherty, *Trends Pharmacol. Sci.* **2002**, *23*, 281 – 287; b) J. C. Ma, D. A. Dougherty, *Chem. Rev.* **1997**, *97*, 1303 – 1324; c) D. A. Dougherty, *Science* **1996**, *271*, 163 – 168; d) D. A. Dougherty, D. A. Stauffer, *Science* **1990**, *250*, 1558 – 1560.

[6] For a review, see: E. A. Meyer, R. K. Castellano, F. Diederich, *Angew. Chem.* **2003**, *115*, 1244 – 1287; *Angew. Chem. Int. Ed.* **2003**, *42*, 1210 – 1250.

[7] K. Schärer, M. Morgenthaler, R. Paulini, U. Obst-Sander, D. W. Banner, D. Schlatter, J. Benz, M. Stihle, F. Diederich, *Angew. Chem.* **2005**, *117*, 4474 – 4479; *Angew. Chem. Int. Ed.* **2005**, *44*, 4400 – 4404.

[8] a) Relibase 2.2.2 (August 2008); b) M. Hendlich, A. Bergner, J. Günther, G. Klebe, *J. Mol. Biol.* **2003**, *326*, 607 – 620; c) J. Günther, A. Bergner, M. Hendlich, G. Klebe, *J. Mol. Biol.* **2003**, *326*, 621 – 636.

[9] a) P. R. Gerber, K. Müller, *J. Comput.-Aided Mol. Des.* **1995**, *9*, 251 – 268; b) Gerber Molecular Design (http://www.moloc.ch).

[10] a) U. Obst, P. Betschmann, C. Lerner, P. Seiler, F. Diederich, V. Gramlich, L. Weber, D. W. Banner, P. Schönhölzer, *Helv. Chim. Acta* **2000**, *83*, 855 – 909; b) E. Schweizer, A. Hoffmann-Röder, P. Schönholzer, K. Schärer, J. A. Olsen, C. Fäh, P. Seiler, U. Obst-Sander, B. Wagner, M. Kansy, F. Diederich, *ChemMedChem* **2006**, *1*, 611 – 621.

[11] a) See the Supporting information; b) M. Nazaré, D. W. Will, H. Matter, H. Schreuder, K. Ritter, M. Urmann, M. Essrich, A. Bauer, M. Wagner, J. Czech, M. Lorenz, V. Laux, V. Wehner, *J. Med. Chem.* **2005**, *48*, 4511 – 4525.

[12] a) J. P. Gallivan, D. A. Dougherty, *Proc. Natl. Acad. Sci. USA* **1999**, *96*, 9459 – 9464; b) R. M. Hughes, M. L. Waters, *J. Am. Chem. Soc.* **2005**, *127*, 6518 – 6519.

[13] We have quantified orthogonal dipolar interactions to be in the range of $\Delta\Delta G = 0.3$ to $0.6\ \mathrm{kcal\,mol^{-1}}$; see for example: F. R. Fischer, W. B. Schweizer, F. Diederich, *Angew. Chem.* **2007**, *119*, 8418 – 8421; *Angew. Chem. Int. Ed.* **2007**, *46*, 8270 – 8273.

[14] S. Tsuzuki, M. Mikami, S. Yamada, *J. Am. Chem. Soc.* **2007**, *129*, 8656 – 8662.

[15] R. M. Hughes, M. L. Benshoff, M. L. Waters, *Chem. Eur. J.* **2007**, *13*, 5753 – 5764.

[16] See for example: a) B. W. Berry, M. M. Elvekrog, C. Tommos, *J. Am. Chem. Soc.* **2007**, *129*, 5308 – 5309; b) M. A. Anderson, B. Ogbay, R. Arimoto, W. Sha, O. G. Kisselev, D. P. Cistola, G. R. Marshall, *J. Am. Chem. Soc.* **2006**, *128*, 7531 – 7541.

